

# Specific heat and magnetic order in $\text{LaMnO}_{3+\delta}$

L. Ghivelder\* and I. Abrego Castillo

*Instituto de Física, Universidade Federal do Rio de Janeiro, C.P.  
68528, Rio de Janeiro, RJ 21945-970, Brazil*

M. A. Gusmão

*Instituto de Física, Universidade Federal do Rio Grande do Sul,  
C.P.15051, Porto Alegre, RS 91501-970, Brazil*

J. A. Alonso

*Instituto de Ciencia de Materiales de Madrid, C.S.I.C., Cantoblanco, 28049  
Madrid, Spain*

L. F. Cohen

*Blackett Laboratory, Imperial College, London SW7 2BZ, United Kingdom*

Magnetic and specific-heat measurements are performed in three different samples of  $\text{LaMnO}_{3+\delta}$ , with  $\delta = 0.11, 0.15$  and  $0.26$ , presenting important disorder effects, such as carrier localization, due to high amounts of La and Mn vacancies. For the samples with  $\delta = 0.11$  and  $0.15$ , magnetic measurements show signatures of a two-step transition: as the temperature is lowered, the system enters a ferromagnetic phase followed by a disorder-induced cluster-glass state. Spin-wave-like contributions and an unexpected large linear term are observed in the specific heat as a function of temperature. In the sample with the highest vacancy content,  $\delta = 0.26$ , the disorder is sufficient to suppress even short-range ferromagnetic order and yield a spin-glass-like state.

75.40.Cx, 75.30.-m, 75.30.Ds

## I. INTRODUCTION

Hole-doped perovskite-type manganese oxides have attracted considerable interest in recent years, motivated by the observation of colossal magnetoresistance (CMR) in numerous related compounds, and the great variety of magnetic and transport properties in this class of materials.<sup>1</sup> Among the La-based systems, the ground state of the stoichiometric parent compound  $\text{LaMnO}_3$  is insulating A-type antiferromagnetic (AF), which is attributed to a cooperative effect of orbital ordering and superexchange interactions.<sup>2</sup> Substitution of a fraction  $x$  of  $\text{La}^{3+}$  by divalent cations such as  $\text{Sr}^{2+}$ ,  $\text{Ca}^{2+}$  or  $\text{Ba}^{2+}$  causes the conversion of a proportional number of  $\text{Mn}^{3+}$  to  $\text{Mn}^{4+}$ . At certain doping ranges ( $0.2 \lesssim x \lesssim 0.5$ ) this induces a metal-insulator transition and the appearance of a ferromagnetic (FM) state. The simultaneous FM and metallic transitions have been qualitatively explained by the double-exchange (DE) model,<sup>3</sup> which considers the magnetic coupling between  $\text{Mn}^{3+}$  and  $\text{Mn}^{4+}$  resulting from the motion of an electron between the two partially filled  $d$  shells. Nevertheless, this DE mechanism does not account for several experimental results, and it has been claimed<sup>4</sup> that a Jahn-Teller type electron-phonon coupling plays an important role in explaining the large magnetoresistive effects.

Conversion of  $\text{Mn}^{3+}$  to  $\text{Mn}^{4+}$  can also be achieved by the presence of non-stoichiometric oxygen in undoped  $\text{LaMnO}_{3+\delta}$ , with a nominal  $\text{Mn}^{4+}$  content of  $2\delta$ . For simplicity this is the crystallographic representation used in

the present work and in most other studies in this system. However, it does not reflect the fact that the system contains randomly distributed La and Mn vacancies rather than oxygen excess, which can not be accommodated interstitially in the lattice.<sup>5</sup> The actual crystallographic formula is better written as  $\text{La}_{1-x}\text{Mn}_{1-y}\text{O}_3$ . By varying the oxygen stoichiometry the resulting compounds display a wide variety of structural and magnetic phases, previously studied by x-rays and neutron scattering,<sup>6,7</sup> as well as magnetic and transport measurements.<sup>6,8</sup> It is well known that the low-temperature magnetic phase of non-stoichiometric  $\text{LaMnO}_{3+\delta}$  changes from AF to FM for small values of  $\delta$  due to the DE interaction caused by the presence of  $\text{Mn}^{4+}$  ions in the sample. However, unlike the cation-doped systems, the material remains insulating at all temperatures, and the FM transition temperature decreases for increasing content of  $\text{Mn}^{4+}$ . The relevant fact to be considered appears to be the competing effect between La vacancies, enhancing the  $\text{Mn}^{3+}$ - $\text{Mn}^{4+}$  DE interaction, and Mn vacancies which introduce considerable disorder in the lattice. For large values of  $\delta$  the FM order is suppressed, and the low-temperature phase is better described by a spin-glass-like state.<sup>6,8</sup>

The competing effect between cation and manganese vacancies makes  $\text{LaMnO}_{3+\delta}$  a model system for studying magnetic interactions and disorder effects in mixed-valence manganites. In order to achieve a better understanding of the low temperature properties of this system we have performed magnetic and specific-heat measurements in three different samples of non-stoichiometric

LaMnO<sub>3+δ</sub>. Magnetic data show signatures of a double transition: as the temperature is lowered, the system first orders ferromagnetically in small weakly-connected clusters, and then changes to a cluster-glass phase. Results of low-temperature specific-heat measurements show an unexpectedly large linear coefficient and a spin-wave contribution. This is interpreted in terms of the existence of disorder-induced charge-localization in these compounds.

## II. EXPERIMENTS

The bulk samples of LaMnO<sub>3+δ</sub> investigated in the present study were thoroughly characterized in Refs. 7–9. They were prepared in polycrystalline form by a citrate technique, as described elsewhere.<sup>7</sup> The products were annealed at 1100 °C in air (Sample 1), 1000 °C in air (Sample 2) and 1000 °C under 200 bar of O<sub>2</sub> (Sample 3). The determination of  $\delta$  was initially performed by thermogravimetric analysis. The final materials were characterized by x-ray diffraction. Neutron powder diffraction diagrams were also collected in the temperature range 2–250 K. The Rietveld method was used to refine the crystal and magnetic structures.

The neutron-diffraction refinements showed that all investigated samples have stoichiometric oxygen content of  $3.00 \pm 0.05$ . The Mn<sup>4+</sup> content was calculated from the vacancy concentration of La and Mn determined from the neutron data, and found to be in good agreement with the thermogravimetric analysis. Sample 1, with  $\delta = 0.11$  and 23% of Mn<sup>4+</sup>, consists of a mixture of a main orthorhombic phase (64%) and a minor rhombohedral phase (36%). Sample 2, with  $\delta = 0.15$  and 33% of Mn<sup>4+</sup>, and Sample 3, with  $\delta = 0.26$  and 52% of Mn<sup>4+</sup>, both have rhombohedral symmetry. Samples 1 and 2 showed a FM ordered structure at low temperatures (with some canting observed in Sample 2), whereas Sample 3 showed spin-glass-like signatures. Transport measurements<sup>8</sup> revealed that all the studied compounds are insulating down to low temperatures, with a typical semiconductor-like behavior. Selected sample parameters are summarized in Table I.

TABLE I. Selected physical parameters and preparation conditions of the LaMnO<sub>3+δ</sub> samples. The actual crystallographic formula is better written as La<sub>1-x</sub>Mn<sub>1-y</sub>O<sub>3</sub>. The FM transition temperature is given by  $T_c$ .

| Sample               | 1             | 2            | 3                      |
|----------------------|---------------|--------------|------------------------|
| $\delta$             | 0.11          | 0.15         | 0.26                   |
| $x, y$               | 0.022, 0.054  | 0.029, 0.069 | 0.029, 0.128           |
| Mn <sup>4+</sup> (%) | 23            | 33           | 52                     |
| Prep. Conditions     | 1100 °C/air   | 1000 °C/air  | 1000 °C/O <sub>2</sub> |
| Cryst. Structure     | Ortho./Rhomb. | Rhomb.       | Rhomb.                 |
| $T_c$ (K)            | 154           | 142          | –                      |

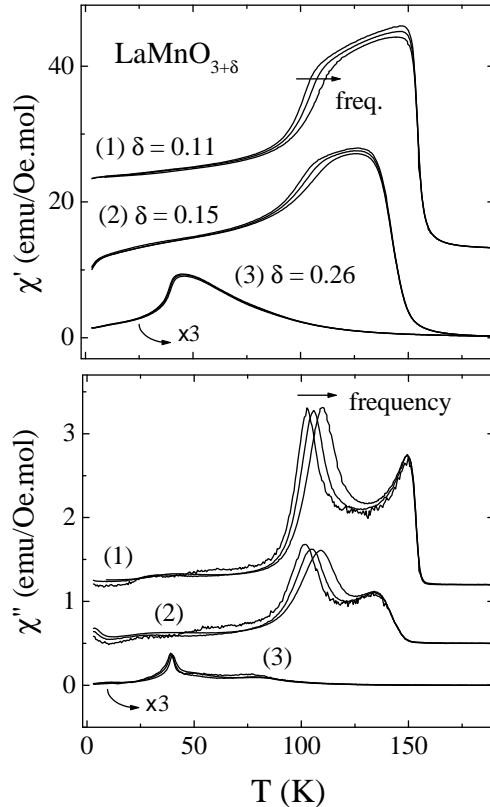


FIG. 1. Real and imaginary parts of the AC susceptibility of LaMnO<sub>3+δ</sub>, measured in an alternating field  $h_{ac} = 1$  Oe and frequencies  $f = 25, 125$  and  $1000$  Hz. For samples with  $\delta = 0.11$  and  $0.15$  (Samples 1 and 2) the data is shifted vertically for clarity. For the sample with  $\delta = 0.26$  (Sample 3) the results are multiplied by 3.

In the present study, specific-heat results were obtained from 4.5 to 200 K with an automated quasi-adiabatic pulse technique. The absolute accuracy of the data, checked against a copper sample, is better than 3%. The measured samples had masses of approximately 50 mg. Detailed AC susceptibility and DC magnetization measurements were performed in a commercial magnetometer (Quantum Design PPMS). The FM transition temperatures of Samples 1 and 2, obtained from AC susceptibility data, are also shown in Table I.

## III. MAGNETIC MEASUREMENTS

Figure 1 shows the AC susceptibility of LaMnO<sub>3+δ</sub>. Real and imaginary parts, respectively  $\chi'$  and  $\chi''$ , were measured in zero DC field, with an alternating field  $h_{ac} = 1$  Oe, and frequencies of 25, 125 and 1000 Hz. Results for Sample 3 are multiplied by a factor of 3. Part

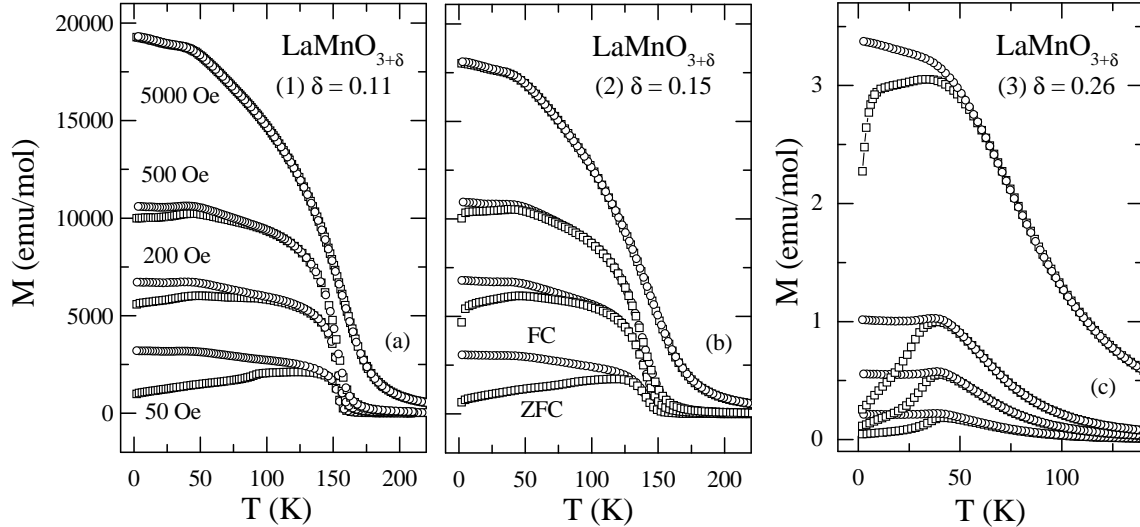


FIG. 2. Field-cooled (FC) and zero-field-cooled (ZFC) DC magnetization of  $\text{LaMnO}_{3+\delta}$ . The applied field, from bottom to top in the figures, is 50, 200, 500 and 5000 Oe.

of the data was shifted vertically for clarity. The first point to note is a pronounced FM transition, observed at 154 and 142 K for Samples 1 ( $\delta = 0.11$ ) and 2 ( $\delta = 0.15$ ), respectively. The values of  $T_c$  were determined from the maximum derivative in  $\chi'$ . For Sample 3, with the higher vacancy content ( $\delta = 0.26$ ), at 48 K we observe a much lower cusp-like anomaly in  $\chi'$ , typical of a spin glass behavior. As mentioned in the introduction, the evolution from FM to spin glass features for increasing oxygen content in  $\text{LaMnO}_{3+\delta}$  was previously observed in the literature.<sup>6,8</sup>

Moreover, it is most interesting to note in Fig. 1 that the results for the two FM samples show a double-peak structure and a frequency dependence of the imaginary component,  $\chi''$ . The high-temperature peak is frequency independent, whereas the position of the low-temperature peak strongly depends on the measuring frequency. The maximum in  $\chi''$  shifts to higher temperatures as the frequency increases. These are clear signatures of a cluster-glass behavior, as previously reported for other manganite<sup>10</sup> and cobaltite<sup>11,12</sup> systems. The high-temperature peak signals the onset of FM order, whereas the low-temperature frequency-dependent peak is associated with freezing of the cluster magnetic moments. In connection with the low-temperature peak in  $\chi''$ , a frequency-dependent shoulder can be observed in the real component  $\chi'$ . Results for Sample 3 also show a distinct frequency dependence in  $\chi'$ , not visible in the scale of the figure.

In order to probe disorder-induced features in the system, we have measured the field-cooled (FC) and zero-field-cooled (ZFC) magnetization of the studied samples. Figures 2(a) and 2(b) display the results for Samples 1 and 2 respectively. The low-field data was taken with

$H = 50$  Oe. A pronounced irreversibility is observed, again indicative of a disordered state. In our results the irreversibility starts just below  $T_c$ , which is the typical behavior of a cluster-glass phase, whereas in reentrant-spin-glass systems irreversibility occurs far below  $T_c$ .

As the field increases the irreversible behavior is reduced, and is no longer present at  $H = 5000$  Oe. Measurements of AC susceptibility with an applied DC field (not shown) confirm that the frequency dependence in  $\chi'$  disappears with increasing fields. These results show that the application of a DC field tends to align the cluster moments, and stabilizes a reversible FM ordered state. In the magnetization results for Sample 3, shown in Fig. 2(c), the behavior is quite different. The magnetization peak is more than two orders of magnitude lower than in the other samples, and the irreversibility persists with higher applied DC field, which confirms the standard spin-glass features in the high-vacancy sample. The difference between the ZFC and FC magnetizations is much higher in the cluster-glass phase (Samples 1 and 2) compared to the spin-glass phase (Sample 3), reflecting the presence of FM order within the clusters.<sup>11</sup>

Isothermal  $M$  vs.  $H$  curves measured at 10 K are plotted in Fig. 3. For the FM samples (1 and 2) the magnetization saturates at fields of the order of 1–2 T. The saturation values are  $3.70 \mu_B$  and  $3.57 \mu_B$  for Samples 1 and 2, respectively. The magnetic moment expected from the spin contribution is  $gS \mu_B$ , where  $S$  is the spin of the ion, which is  $3/2$  for  $\text{Mn}^{4+}$  and  $2$  for  $\text{Mn}^{3+}$ , and the gyromagnetic factor  $g = 2$  in both cases. Taking into account the relative concentrations of  $\text{Mn}^{4+}$  and  $\text{Mn}^{3+}$  in the compounds, we get an effective moment of  $3.77 \mu_B$  for Sample 1 (23%  $\text{Mn}^{4+}$ ), and  $3.67 \mu_B$  for Sample 2 (33%

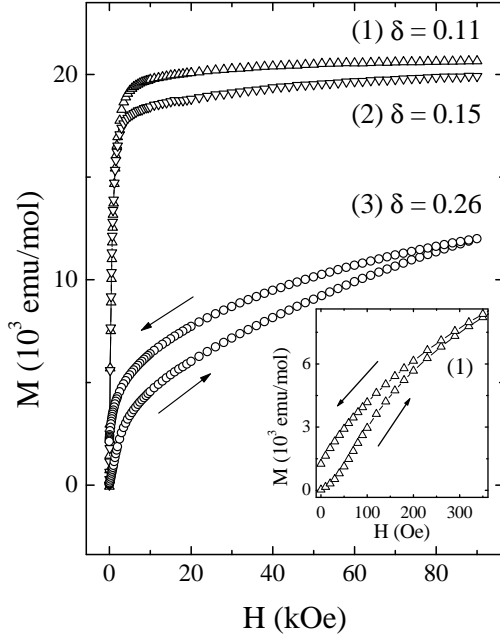


FIG. 3. Magnetization as a function of field of  $\text{LaMnO}_{3+\delta}$ , measured at 10 K. The inset shows low-field data for Sample 1. The arrows indicate measurements increasing and decreasing the field.

$\text{Mn}^{4+}$ ). This prediction virtually coincides with the values observed experimentally, indicating that the applied field fully polarizes the FM clusters. Hysteresis is observed at very low fields, up to about 400 Oe, as shown for Sample 1 in the inset of Fig. 3. This hysteresis is consistent with the  $M$  vs.  $T$  data of Fig. 2, and is attributed to the low field cluster-glass nature of the samples. For Sample 3 (52%  $\text{Mn}^{4+}$ ), the low-temperature magnetization does not saturate at our highest field, and a large hysteretic behavior is observed. At 9 T the measured magnetic moment is  $2.15 \mu_B$ , much smaller than the predicted value of  $3.48 \mu_B$ . This is an additional indication of the spin-glass-like properties of this sample.

In order to verify the consistency of our magnetic results, we have performed the same measurements on another similar series of  $\text{LaMnO}_{3+\delta}$  samples. The cluster-glass behavior of the intermediate-vacancy FM samples, i.e., the frequency-dependent AC susceptibility and the irreversibility in low-field magnetization, were confirmed to exist in this second series of samples.

#### IV. SPECIFIC HEAT MEASUREMENTS

Figure 4(a) shows the specific heat of the investigated samples plotted as  $C/T$  vs.  $T^2$ , in the temperature range of 4.5–15 K. For comparison, measurements on  $\text{La}_{0.90}\text{Ca}_{0.10}\text{MnO}_3$ , a ferromagnetic insulator, and on  $\text{La}_{0.67}\text{Ca}_{0.33}\text{MnO}_3$ , a ferromagnetic metal, are also

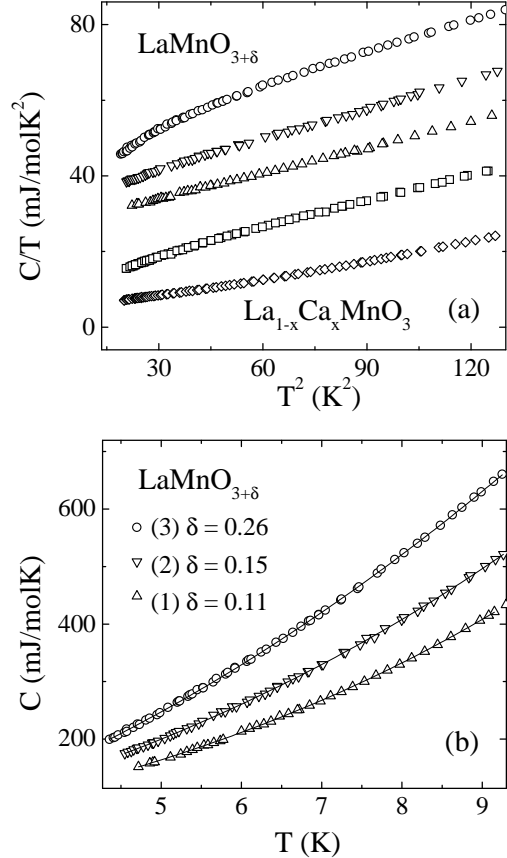


FIG. 4. (a) From top to bottom, low-temperature specific heat, plotted as  $C/T$  vs.  $T^2$ , for  $\text{LaMnO}_{3+\delta}$  with  $\delta = 0.26$  (circles), 0.15 (down triangles), and 0.11 (up triangles), and for  $\text{La}_{1-x}\text{Ca}_x\text{MnO}_3$  with  $x = 0.11$  (squares) and 0.33 (diamonds). (b) Plot of  $C$  vs.  $T$  for  $\text{LaMnO}_{3+\delta}$ ; the solid lines are fitted curves, as discussed in the text.

displayed.<sup>13</sup> The latter has the same  $\text{Mn}^{4+}$  content as in  $\text{LaMnO}_{3+\delta}$  with  $\delta = 0.15$ . However, it is clear from the figure that the heat capacity is considerably higher in  $\text{LaMnO}_{3+\delta}$  as compared to the Ca-doped compounds. In order to interpret these results and evaluate the different contributions to the specific heat, the low-temperature data of each studied sample were fitted to the expression

$$C = \gamma T + \beta T^3 + BT^{3/2}. \quad (1)$$

The linear coefficient  $\gamma$  is usually attributed to charge carriers, and is proportional to the density of states at the Fermi level. However, transport measurements showed that all the investigated samples of  $\text{LaMnO}_{3+\delta}$  are insulating, and the appearance of a linear term in the specific heat must be more carefully interpreted. The lattice contribution is given by  $\beta T^3$ . A higher-order lattice term proportional to  $T^5$  was not needed to fit the data in the temperature range up to 10 K. The term  $BT^{3/2}$  is associated with FM spin-wave excitations. The coefficient

TABLE II. Fitting results of the low-temperature specific heat of  $\text{LaMnO}_{3+\delta}$ . The linear coefficient is given by  $\gamma$ . The Debye temperature  $\theta_D$  is obtained from the cubic coefficient  $\beta$ , and the spin-wave stiffness constant  $D$  is obtained from the magnetic term  $BT^{3/2}$ .

| Sample                | $\gamma$ (mJ/mol K <sup>2</sup> ) | $\beta$ (mJ/mol K <sup>4</sup> ) | $\theta_D$ (K) | $B$ (mJ/mol K <sup>5/2</sup> ) | $D$ (meVÅ <sup>2</sup> ) |
|-----------------------|-----------------------------------|----------------------------------|----------------|--------------------------------|--------------------------|
| 1 ( $\delta = 0.11$ ) | $23 \pm 3$                        | $0.193 \pm 0.02$                 | $369 \pm 13$   | $2.1 \pm 0.6$                  | $75 \pm 15$              |
| 2 ( $\delta = 0.15$ ) | $19 \pm 2$                        | $0.168 \pm 0.02$                 | $387 \pm 15$   | $7.5 \pm 1.0$                  | $32 \pm 3$               |
| 3 ( $\delta = 0.26$ ) | 0                                 | $0.0786 \pm 0.007$               | $498 \pm 15$   | $21.2 \pm 0.2$                 | $16.1 \pm 0.1$           |

$\beta$  is related to the Debye temperature  $\theta_D$ , and the coefficient  $B$  to the spin-wave stiffness constant  $D$ .<sup>14</sup>

The fitting parameters obtained for all samples are given in Table II, and the fitted curves can be seen in Fig. 4(b) in a plot of  $C$  vs.  $T$ . For Samples 1 and 2 ( $\delta = 0.11$  and  $0.15$ ) although the plot of  $C/T$  vs.  $T^2$  gives approximately straight lines, a careful fitting procedure confirms the existence of a magnetic  $BT^{3/2}$  term. The uncertainty in the coefficients is estimated mostly by varying the fitted temperature range. All fitted curves fall within the experimental data with a maximum dispersion smaller than  $\pm 0.7\%$  in more than 90% of the points, and no systematic departures from the fitted curves are observed. In Sample 3 ( $\delta = 0.26$ ) we found no contribution arising from a linear term  $\gamma T$ . An upper estimate gives  $\gamma < 0.8$  mJ/mol K<sup>2</sup>, obtained using a maximum fitting temperature above 9 K. Below this range, the inclusion of a linear term in the fitted expression yields negative values of  $\gamma$ . By allowing the magnetic contribution to vary as  $BT^n$

we find a best fit with  $n$  very close to the assumed value of  $3/2$ . One of the most important and unexpected results obtained from our low-temperature specific-heat data is the observation of a very high linear coefficient  $\gamma$  in Samples 1 and 2. In this case, by fitting the data only with linear and cubic terms we obtain even higher values of  $\gamma$ . Possible origins of this contribution will be discussed below.

The Debye temperature  $\theta_D$  significantly increases with the increase of vacancy content in  $\text{LaMnO}_{3+\delta}$ . The values of  $\theta_D$ , in the range 370-500 K, are comparable to those previously reported in manganite perovskites.<sup>13,15-18</sup> The tendency to an increase of  $\theta_D$  with higher hole doping has been previously observed.<sup>13,17,18</sup> It has been argued<sup>18</sup> that the reduction of lattice stiffness at low doping values could be related to dynamic Jahn-Teller distortion in the compounds. The large value of  $\theta_D$  in Sample 3, with the highest content of  $\text{Mn}^{4+}$ , is close to that observed<sup>13</sup> in the AF insulator  $\text{La}_{0.38}\text{Ca}_{0.62}\text{MnO}_3$ . This suggests that AF interactions, also present in Sample 3, may contribute to a hardening of the lattice vibrations.

The magnitude of the  $BT^{3/2}$  term is also of relevance, providing information on the spin-wave excitations in the compounds. The value of the spin-wave stiffness constant determined for Sample 1,  $D = 75 \text{ meV}\text{\AA}^2$ , is approximately half of that obtained for  $\text{La}_{0.7}\text{Ca}_{0.3}\text{MnO}_3$  ( $D = 170 \text{ meV}\text{\AA}^2$ )<sup>19</sup> and  $\text{La}_{0.7}\text{Sr}_{0.3}\text{MnO}_3$  ( $D = 154 \text{ meV}\text{\AA}^2$ ),<sup>20</sup> both in the FM metallic phase. The value of  $D = 32 \text{ meV}\text{\AA}^2$  in Sample 2 is of the same order as in the FM insulator  $\text{La}_{0.9}\text{Ca}_{0.1}\text{MnO}_3$  ( $D = 40 \text{ meV}\text{\AA}^2$ ),<sup>13</sup> whose insulating character is also interpreted as a disorder effect. This is consistent with the fact that increasing disorder should give rise to lower values of  $D$ , i.e., “softer” spin waves, as it is expected to reduce the strength of the ferromagnetic coupling. The observation of a magnetic  $BT^{3/2}$  contribution in Sample 3, for which a spin-glass phase is observed, will be addressed in the next section.

For completeness, Fig. 5 displays the high-temperature (30–200 K) specific heat of the investigated  $\text{LaMnO}_{3+\delta}$  samples, plotted as  $C/T$  vs.  $T$ . Results for Samples 2 and 3 are shifted downward for clarity, as indicated by the arrows. Sample 1 shows a small anomaly associated with the FM transition at 152 K, coinciding with the transition temperature obtained from the AC susceptibility. No anomaly is observed in the results for Samples 2 and 3. The inset shows the temperature derivative,  $d(C/T)/dT$ , for Samples 1 and 2. The FM transition in Sample 2 is visible in the derivative plot at 143 K, again coinciding with the sus-

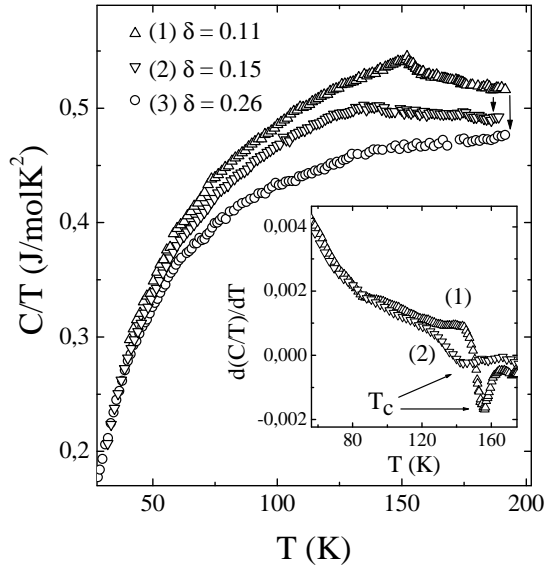


FIG. 5. High-temperature (30–200 K) specific heat of  $\text{LaMnO}_{3+\delta}$ , plotted as  $C/T$  vs.  $T$ . Results for Samples 2 and 3 are shifted downward for clarity, as indicated by the arrows. The inset shows the temperature derivative  $d(C/T)/dT$  vs.  $T$  for Samples 1 and 2, with the FM transition temperatures indicated.

ceptibility measurements. Phase transitions with a large temperature width often show no specific-heat anomaly, as reported<sup>13</sup> in the FM insulator  $\text{La}_{0.90}\text{Ca}_{0.10}\text{MnO}_3$ . For Sample 3, a specific-heat anomaly is not observed even in the derivative plot (not shown), as expected for a spin glass. For Sample 1, the entropy associated with the FM transition, which can be obtained from  $\Delta S = \int (C/T)dT$ , is  $\Delta S = 0.21 \pm 0.02$  J/molK. The subtracted lattice contribution is estimated by excluding the peak region from the data, and fitting the remaining data with a sum of three Einstein optical modes. The value of  $\Delta S$  is about an order of magnitude smaller than reported on Ca-doped samples,<sup>13,21</sup> and on other manganite compounds,<sup>22,23</sup> where in turn the  $\Delta S$  values are also smaller than expected from the ordering of the spin system. A thorough discussion related to this “missing” entropy can be found elsewhere.<sup>23</sup>

## V. DISCUSSION

From our susceptibility and magnetization data we have established that the FM phase of hole doped  $\text{LaMnO}_{3+\delta}$  samples evolves to a cluster-glass-like state. Several other manganite compounds present similar behavior when substitution occurs in the manganese site. If one takes, for instance, the standard CMR compound  $\text{La}_{0.7}\text{Ca}_{0.3}\text{MnO}_3$ , substitution of Mn by Co (Ref. 24) or In (Ref. 25) also gives rise to an insulating cluster-glass phase. This suggests that the DE interaction, mostly responsible for the metallic FM state of doped manganites, is inhibited by random disorder in the system. The formation of FM clusters is accompanied by strong charge-localizing effects which yield an insulating state. Nevertheless, the size of the clusters must be large enough for the  $e_g$  electrons to extend over several sites, and provide the observed FM interaction.

The most striking feature of the specific-heat data for Samples 1 and 2 is the appearance of an unexpectedly large linear term, in excess of 19 mJ/molK<sup>2</sup>, although the system as whole is an insulator with respect to transport properties. It is most important to understand the origin of this anomalous contribution. Compared with the increasing number of publications on doped manganite perovskite samples, relatively few reports on heat capacity have been presented. Low-temperature data for  $\text{LaMnO}_3$  doped with Ca,<sup>13,15,16</sup> Sr,<sup>16,17</sup> and Ba,<sup>15,16</sup> all in the metallic FM phase, observed a specific-heat linear term  $\gamma$  in the range of 5–7 mJ/molK<sup>2</sup>, associated with conduction electrons. However, few previous investigations have reported high  $\gamma$  values in insulating manganite samples: in the electron doped system  $\text{La}_{2.3}\text{Ca}_{0.7}\text{Mn}_2\text{O}_7$ ,<sup>26</sup> the authors found  $\gamma = 41$  mJ/molK<sup>2</sup>, and in  $\text{Nd}_{0.67}\text{Sr}_{0.33}\text{MnO}_3$ <sup>22</sup> a value of  $\gamma = 25$  mJ/molK<sup>2</sup> was observed. A detailed explanation for this contribution has not been put forward. As already mentioned, our magnetic results clearly allow us to infer

that ferromagnetic order in  $\text{LaMnO}_{3+\delta}$  develops in regions of limited size (clusters), whose magnetic moments undergo a spin-glass-like transition. We will argue now that our heat capacity results are consistent with this picture.

The stoichiometric compound  $\text{LaMnO}_3$  ( $\delta = 0$ ) has an orthorhombic crystal structure,<sup>27</sup> which is a distorted form of the cubic perovskite structure. The ideal cubic system would have a FM metallic character, with the Fermi energy lying in the middle of the  $e_g$  band.<sup>28</sup> The splitting of the  $e_g$  bands, due to the Jahn-Teller distortion, leads to a small gap (1.5 eV) between the Mn  $e_g^1$  and  $e_g^2$  bands. This stabilizes the A-type AF order and makes the system a Mott insulator. As we dope with holes,  $\text{Mn}^{4+}$  are created, the perovskite distortion decreases, and the Fermi level drops down into the lowest half of the split band. Thus the system becomes metallic, with the DE mechanism being responsible for charge transfer among Mn ions, and the consequent polarization of the  $t_{2g}$  spins that yield ferromagnetic order. However, in non-stoichiometric  $\text{LaMnO}_{3+\delta}$ , the disorder introduced by random La and Mn vacancies may cause Anderson-like localization of the electron states close to the band edges. In contrast to what happens in the cation-substituted compounds, the disordering effect of Mn vacancies is strong enough for localization to be effective even at high concentrations of  $\text{Mn}^{4+}$ .

Previous theoretical investigations<sup>29–31</sup> confirmed that disorder leads to charge localization in doped manganites. As is well known since Anderson’s original paper,<sup>32</sup> a distribution of site-dependent diagonal energies produces localization of the electronic states from the edges of the bands to an energy within them which is called the *mobility edge*. Allub and Alascio<sup>29,30</sup> have shown that, for  $\text{La}_{1-x}\text{Sr}_x\text{MnO}_3$ , according to the amount of disorder and concentration of carriers, the Fermi level can cross the mobility edge to produce a metal-insulator transition. Disorder is quantified by a distribution width  $\Gamma$ . If  $\Gamma$  is large, charge localization is enhanced, and the system remains insulating, as observed in our  $\text{LaMnO}_{3+\delta}$  samples. It is worth mentioning that electron localization also occurs in metallic manganite compounds. It has been argued<sup>16</sup> that the  $e_g$  electrons may be localized in large wave packets due to potential fluctuations arising from cation substitution, and additionally by spin-dependent fluctuations due to local deviations from FM order. In  $\text{LaMnO}_{3+\delta}$  the missing Mn ions enhance these random fluctuations, favoring charge localization.<sup>33</sup>

On the other hand, it is reasonable to assume that at low vacancy concentration the Fermi level does not fall too far above the mobility edge, which implies that the localization length may be fairly large. Charge carriers can thus hop between a number of Mn ions, which actually defines the FM clusters. The electron mobility inside the clusters ensures the effectiveness of the DE interaction, giving rise to the observed FM behavior. Furthermore, if the FM regions are not too small, regular spin waves can

be excited inside them, yielding the observed  $T^{3/2}$  contribution to the specific heat. This is consistent with the values obtained for the spin wave stiffness in these compounds. The electron levels, although localized, are not largely spaced in energy, allowing for thermal excitations that contribute with a linear term to the specific heat as a function of temperature. It remains to be understood why the coefficient of the specific-heat linear term is so large in our results, as compared to other perovskite systems. A number of mass enhancement mechanisms may be envisaged, like magnetic polarons, lattice polarons related to the dynamical Jahn-Teller effect, or Coulomb interaction effects. However, it is not straightforward to understand why these effects would not be equally noticeable in most doped manganite compounds. We suggest that the explanation lies in the fact that localization has changed the Fermi level to a region of high density of states. For instance, it is possible that the disorder yields an enhancement of the two-dimensional character of the bands, giving rise to a high density of states. Indeed, band structure calculations<sup>28,34</sup> on stoichiometric  $\text{LaMnO}_3$  revealed sharp features resembling the typical logarithmic van Hove singularities of two-dimensional tight-binding bands.

Sample 3, with the largest vacancy content, shows qualitatively distinct characteristics. Nevertheless, its behavior can be interpreted with the same arguments discussed above. The localization length is now very small due to the high degree of disorder. Thus, FM clusters are no longer formed, which is consistent with the observed magnetic response of the compound. The absence of a linear term in the specific heat reflects the higher degree of localization of the charge carriers, which effectively prevents the DE mechanism. The system behavior closely resembles that of a regular spin glass, with short range FM interaction competing with AF coupling, the latter arising from the high  $\text{Mn}^{4+}$  content. It is somewhat puzzling, though, that the dominant contribution to the specific heat is a term proportional to  $T^{3/2}$ , which is usually attributed to spin waves in a long range FM system. However, according to computer simulations by Walker and Walstedt<sup>35</sup> on a model spin glass, the low-energy excitations are collective modes, even though the local magnetic moments do not show long range order. Thus, some power-law behavior of the specific heat with temperature can be expected. Linear and quadratic terms are obtained in Ref. 35 for a model metallic spin glass with RKKY interactions, but the actual value of the exponent depends on details of the distribution of low-lying excitations, and a value of  $3/2$  cannot be ruled out.

## VI. CONCLUSIONS

In this work we have presented measurements of AC susceptibility, DC magnetization, and specific heat in a series of  $\text{LaMnO}_{3+\delta}$  samples with large  $\delta$  values, and

therefore high degree of disorder. The aim is to provide a better understanding of the role of La and Mn vacancies in the properties of mixed-valence manganites. From our analysis we may draw two main conclusions: (i) magnetic measurements showed that the previously known FM insulating phase of these compounds displays a disorder-induced cluster-glass-like behavior; (ii) the anomalous high specific-heat linear coefficient  $\gamma$  in this case gives evidence of a high density of localized states around the Fermi level, even though the latter falls in a region of Anderson-localized states. Hence, charge localization is enhanced due to disorder in the system, and the low temperature FM insulating state consists of randomly oriented FM clusters, which align in small applied fields. The carriers, though localized, may hop between several Mn sites to ensure the DE interaction responsible for the FM order. In the sample with the highest vacancy content the increased random disorder, and the competition between FM and AF interactions give rise to a spin-glass state.

## VII. ACKNOWLEDGMENTS

We thank Mucio Continentino and Gerardo Martínez for helpful discussions. This research was financed by the Brazilian Ministry of Science and Technology under the contract PRONEX/FINEP/CNPq no 41.96.0907.00. Additional support was also given by FUJB and FAPERJ. J.A.A. thanks the Spanish CICYT for funds to the project PB97-1181. L.F.C. was supported by the EPSRC grant number GR/K 73862 and by the Royal Society, U.K.

---

\* Corresponding author; e-mail: huiqghiv@if.ufrj.br.

<sup>1</sup> For a comprehensive review, see *Colossal Magneto Resistance, Charge Ordering and Related Properties of Manganese Oxides*, edited by C.N.R. Rao and B. Raveau (World Scientific, Singapore, 1998).

<sup>2</sup> S. Ishihara, J. Inoue, and S. Maekawa, *Phys. Rev. B* **55**, 8280 (1997); A. J. Millis, *Phys. Rev. B* **55**, 6405 (1997).

<sup>3</sup> C. Zener, *Phys. Rev.* **81**, 440 (1951).

<sup>4</sup> A. J. Millis, B. I. Shraiman, and R. Mueller, *Phys. Rev. Lett.* **77**, 175 (1996); H. Röder, Jun Zang, and A. R. Bishop, *Phys. Rev. Lett.* **76**, 1356 (1996).

<sup>5</sup> J.A.M. Van Roosmalen and E.H.P. Cordfunke, *J. Solid State Chem.* **110**, 106 (1994).

<sup>6</sup> C. Ritter, M. R. Ibarra, J. M. De Teresa, P. A. Algarabel, C. Marquina, J. Blasco, J. García, S. Oseroff, and S-W. Cheong, *Phys. Rev. B* **56**, 8902 (1997).

<sup>7</sup> J.A. Alonso, M.J. Martínez-Lope, M.T. Casais, J.L. MacManus-Driscoll, P.S.I.P.N. de Silva, and L.F. Cohen, *J. Mater. Chem.* **7**, 2139 (1997).

- <sup>8</sup> P.S.I.P.N. de Silva, F.M. Richards, L.F. Cohen, J.A. Alonso, M.J. Martinez-Lope, M.T. Casais, K.A. Thomas, and J.L. MacManus-Driscoll, *J. Appl. Phys.* **83**, 394 (1998).
- <sup>9</sup> J.A. Alonso, M.J. Martinez-Lope, M.T. Casais, and A. Muñoz, *Solid State Commun.* **102**, 7 (1997).
- <sup>10</sup> A. Maignan, C. Martin, F. Damay, B. Raveau, and J. Hejtmanek, *Phys. Rev. B.* **58**, 2758 (1998).
- <sup>11</sup> S. Mukherjee, R. Ranganathan, P.S. Anilkumar, and P.A. Joy, *Phys. Rev. B.* **54**, 9267 (1996).
- <sup>12</sup> D.H.N. Nam, K. Jonason, P. Nordblad, N.V. Khiem, and N.X. Phuc, *Phys. Rev. B.* **59**, 4189 (1999).
- <sup>13</sup> L. Ghivelder, I. Abrego Castillo, N. McN. Alford, G.J. Tomka, P. C. Riedi, J. MacManus-Driscoll, A.K.M. Akther Hossain, and L.F. Cohen, *J. of Magn. Magn. Mater.* **189**, 274 (1998).
- <sup>14</sup> E.S.R. Gopal, *Specific Heat at Low Temperatures* (Plenum, New York, 1966); C. Kittel, *Quantum Theory of Solids* (Wiley, New York, 1987).
- <sup>15</sup> J.J. Hamilton, E.L. Keatley, H.L. Ju, A.K. Raychaudhuri, V.N. Smolyaninova, and R.L. Greene, *Phys. Rev. B* **54**, 14926 (1996).
- <sup>16</sup> J.M.D. Coey, M. Viret, L. Ranno, and K. Ounadjela, *Phys. Rev. Lett.* **75**, 3910 (1995).
- <sup>17</sup> B.F. Woodfield, M.L. Wilson, and J.M. Byers, *Phys. Rev. Lett.* **78**, 3201 (1997).
- <sup>18</sup> T. Okuda, A. Asamitsu, Y. Tomioka, T. Kimura, Y. Taguchi, and Y. Tokura, *Phys. Rev. Lett.* **81**, 3203 (1998).
- <sup>19</sup> J.W. Lynn, R.W. Erwin, J.A. Borchers, Q. Huang, A. Santoro, J.L. Peng, and Z.Y. Li, *Phys. Rev. Lett.* **76**, 21, 4046 (1996).
- <sup>20</sup> V.N. Smolyaninova, J.J. Hamilton, R.L. Greene, Y.M. Mukovskii, S.G. Karabashev and A.M. Balbashov, *Phys. Rev. B* **55**, 5640 (1997).
- <sup>21</sup> J. Tanaka and T. Mitsuhashi, *J. Phys. Soc. Jpn.* **53**, 24 (1983).
- <sup>22</sup> J.E. Gordon, R.A. Fisher, Y.X. Jia, N.E. Phillips, D.A. Wright, and A. Zettl, *Phys. Rev. B* **59**, 127 (1999).
- <sup>23</sup> M.R. Lees, O.A. Petrenko, G. Balakrishnan, and D. McK. Paul, *Phys. Rev. B* **59**, 1298 (1999).
- <sup>24</sup> N. Gayathri, A.K. Raychaudhuri, S.K. Tiwary, R. Gundakaram, A. Arulraj, and C.N.R. Rao, *Phys. Rev. B* **56**, 1345 (1997).
- <sup>25</sup> M.C. Sanchez, J. Blasco, J. Garcia, J. Stankiewicz, J.M. De Teresa and M.R. Ibarra, *J. Solid State Chem.* **138**, 226 (1998).
- <sup>26</sup> P. Raychaudhuri, C. Mitra, A. Paramekanti, R. Pinto, A.K. Nigam, and S.K. Dhar, *J. Phys.: Condens. Matter* **10**, L191 (1998).
- <sup>27</sup> J.B.A.A. Elemans, B. van Laar, K.R. van der Veen, and B.O. Loopstra, *J. Solid State Chem.* **3**, 238 (1971).
- <sup>28</sup> S. Satpathy, Z.S. Popovic, and F.R. Vukajlović, *Phys. Rev. Lett.* **76**, 960 (1996).
- <sup>29</sup> R. Allub and B. Alascio, *Solid State Commun.* **99**, 613 (1996).
- <sup>30</sup> R. Allub and B. Alascio, *Phys. Rev. B* **55**, 14113 (1997).
- <sup>31</sup> C.M. Varma, *Phys. Rev. B* **54**, 7328 (1996).
- <sup>32</sup> P.W. Anderson, *Phys. Rev.* **109**, 1492 (1958).
- <sup>33</sup> L. Ranno, M. Viret, R.M. Thomas, and J.M.D. Coey, *J. Phys.: Condens. Matter* **8**, L33 (1996).
- <sup>34</sup> D.J. Singh and W.E. Pickett, *J. Appl. Phys.* **83**, 7354 (1998).
- <sup>35</sup> L.R. Walker and R.E. Walstedt, *Phys. Rev. Lett.* **38**, 514 (1977).